

<sup>(d)</sup>Permanent address: University of Tokyo, Tokyo, Japan.

<sup>(e)</sup>Now at Physikalisches Institut, Technische Hochschule Aachen, Aachen, Germany.

<sup>1</sup>For  $\pi^0$  correlations, see K. Eggert *et al.*, Nucl. Phys. **B98**, 49 (1975); F. W. Büsser *et al.*, Phys. Lett. **51B**, 311 (1974). For charged-particle correlations, see M. Della Negra *et al.*, CERN Report No. CERN/EP/PHYS77-10 (to be published); see also recent reviews by G. C. Fox and H. J. Frisch, Brookhaven National Laboratory Report No. BNL-50598, edited by H. Gordon and R. F. Peierls, Proceedings of the American Physical Society Meeting, Division of Particles and Fields, Upton, New York, 1976 (unpublished); by H. Bøggild, in Proceedings of the Seventh International Symposium on Multiparticle Dynamics, Kayserberg, June 1977 (unpublished); by M. Della Negra, in Proceedings of the European Conference on Particle Physics at Budapest, July 1977 (unpublished).

<sup>2</sup>C. Kourkoumelis, CERN Report No. CERN 77-06 (unpublished); J. H. Cobb *et al.*, Phys. Lett. **68B**, 101 (1977).

<sup>3</sup>Although we have taken data by separate trigger with acceptance at smaller angles, their analysis is not yet complete.

<sup>4</sup>A more certain, but biased  $\pi^0$  definition requires two reconstructed photons with  $\pi^0$  effective mass. However, this definition yields poor efficiency at high  $P_T$ . When two reconstructed showers coexist in the same octant, the  $\pi^0$  energy was taken as that of the highest-energy shower. The inclusion of the lower-energy shower or

additional nearby energy in the  $\pi^0$  definition has no significant effect on our results.

<sup>5</sup>The spectrum has been weighted for geometrical and energy efficiency as determined by calibration runs at the CERN proton synchrotron so that the two  $\pi^0$ 's, when given random angles would have a flat distribution, independent of transverse momentum above  $P_T = 1.2$  GeV/c. Trigger corrections due to the ISR intersection angle have been made. The weight of an event varies from 0.3 to 3, with an average weight of 1.

<sup>6</sup>We have also examined the product  $\Pi = P_{T_1} \cdot P_{T_2} \cdot P_{TC}$ . We find distributions similar to those of the  $E_T$  selection.

<sup>7</sup>C. Michael and L. Vanryckeghem, University of Liverpool Report No. LTH 31, May 1977 (to be published), and private communication. We compared our spectrum in  $\Delta\varphi$  with that predicted by the independent-emission model for events with  $9 < E_T < 12$  GeV and  $P_{T_1} > 1$  GeV;  $P_{T_2} > 3$  GeV. The 412 events in our sample have a distribution essentially the same as that of Fig. 2(b). The model predicts a nearly uniform distribution with variations of  $< 20\%$  over our azimuthal coverage.

<sup>8</sup>The diplot of Fig. 3 is not corrected for efficiency which varies by less than 30% in the populated regions.

<sup>9</sup>Recent measurements of  $\Upsilon(9.5) \rightarrow e^+e^-$  in the same apparatus [J. H. Cobb *et al.*, Phys. Lett. **72B**, 273 (1977)], combined with an assumed 3% branching ratio to electrons, would indicate that there are several hundred decays of  $\Upsilon(9.5)$  to hadrons in the data sample from which the present events are drawn.

## Atomic Electron Correlation in Nuclear Electron Capture

Mau Hsiung Chen and Bernd Crasemann

Department of Physics, University of Oregon, Eugene, Oregon 97403

(Received 21 February 1978)

The effect of electron-electron Coulomb correlation on orbital-electron capture by the nucleus has been treated by the multiconfigurational Hartree-Fock approach. The theoretical  ${}^7\text{Be}$   $L/K$  capture ratio is found to be 0.086, and the  ${}^{37}\text{Ar}$   $M/L$  ratio, 0.102. Both ratios are smaller than the independent-particle predictions. Measurements exist for the  $\text{Ar}$   $M/L$  ratio, and agreement between theory and experiment is excellent.

Benoist-Gueutal's insight<sup>1</sup> that atomic electrons must be included in a complete description of orbital-electron capture by the nucleus<sup>2</sup> led to the introduction of atomic exchange and imperfect-overlap factors in the theoretical capture probability.<sup>3-6</sup> All existing work on electron capture has been carried out in the independent-particle approximation; effects due to electron-electron Coulomb correlation have been neglected. Here we report on a first effort to take correlation into account, by using the multiconfigurational Hartree-Fock (MCHF) approach.<sup>7</sup> We calculate the  ${}^7\text{Be}$   $L/K$  and  ${}^{37}\text{Ar}$   $M/L$  capture ratios.

The nuclear-electron-capture rate is<sup>2</sup>

$$\lambda_i = \lambda_i^0 B_i, \quad i = K, L, M, \dots, \quad (1)$$

where  $\lambda_i^0$  is the rate obtained when atomic matrix elements are neglected,<sup>8</sup> and  $B_i$  is the exchange-

overlap correction factor. For example, if the initial and final states are represented by a single Slater determinant, then

$$B_k = K \{ \langle 2s' | 2s \rangle \langle 3s' | 3s \rangle - \langle 2s' | 1s \rangle \langle 3s' | 3s \rangle [R_{2s}(0)/R_{1s}(0)] - \langle 2s' | 2s \rangle \langle 3s' | 1s \rangle [R_{3s}(0)/R_{1s}(0)] \}^2, \quad (2)$$

where

$$K = \langle 1s' | 1s \rangle^2 \langle 2s' | 2s \rangle^2 \langle 2p' | 2p \rangle^{2q(2p)} \langle 3s' | 3s \rangle^{2[q(3s)-1]} \langle 3p' | 3p \rangle^{2q(3p)}. \quad (3)$$

Here,  $q(nl)$  is the occupation number of the  $nl$  shell, and primes denote the daughter atom. Bahcall<sup>2-6</sup> set  $K=1$ , while Vatai<sup>2,9</sup> retained the factor. Similar expressions exist for  $B_L$  and  $B_M$ .

The capture ratio for shells  $i$  and  $j$ , in allowed transitions, is<sup>2</sup>

$$(\lambda_i/\lambda_j) = (\lambda_i/\lambda_j)^0 (B_i/B_j), \quad (4)$$

where

$$(\lambda_i/\lambda_j)^0 = [R_i^2(0)/R_j^2(0)] (q_i^2/q_j^2), \quad (5)$$

$$i, j = K, L_1, M_1.$$

The  $R$ 's are electron radial wave functions, evaluated at the origin, and the  $q$ 's are neutrino energies. The contributions from  $L_2$  and  $M_2$  electrons are neglected here.

In our MCHF calculation, the ground state is

$$\Psi_g(\gamma LS) = \sum_i C_i \Phi(\gamma_i LS), \quad (6)$$

and the final-state wave function, describing the hole state after capture, is

$$\Psi_j'(\gamma LS) = \sum_i C_{ji}' \Phi_i'(\gamma_i LS). \quad (7)$$

$$\begin{aligned} \Psi_g = & C_1 \Phi_1(1s^2 2s^2 2p^6 3s^2 3p^6) + C_2 \Phi_2(1s^2 2s^2 2p^6 3p^6 3d^2(1S)) + C_3 \Phi_3(1s^2 2s^2 2p^6 3s^2 3p^4(1S) 3d^2(1S)) \\ & + C_4 \Phi_4(1s^2 2s^2 2p^6 3s^2 3p^4(3P) 3d^2(3P)) + C_5 \Phi_5(1s^2 2s^2 2p^6 3s^2 3p^4(1D) 3d^2(1D)). \end{aligned} \quad (13)$$

The 2s-hole state is

$$\begin{aligned} \Psi_j = & C_{j1} \Phi_1'(1s^2 2s 2p^6 3s^2 3p^6) + C_{j2} \Phi_2'(1s^2 2s 2p^6 3s^2 3p^4(1S) 3d^2(1S)) + C_{j3} \Phi_3'(1s^2 2s 2p^6 3s^2 3p^4(3P)^2 P 3d^2(3P)) \\ & + C_{j4} \Phi_4'(1s^2 2s 2p^6 3s^2 3p^4(3P)^2 P 3d^2(3P)) + C_{j5} \Phi_5'(1s^2 2s 2p^6 3s^2 3p^4(1D) 3d^2(1D)). \end{aligned} \quad (14)$$

The 3s-hole state after  $M_1$  capture is

$$\begin{aligned} \Psi_j = & C_{j1} \Phi_1'(1s^2 2s^2 2p^6 3s 3p^6) + C_{j2} \Phi_2'(1s^2 2s^2 2p^6 3s^2 3p^4(1D) 3d) + C_{j3} \Phi_3'(1s^2 2s^2 2p^6 3s 3p^4(1S) 3d^2(1S)) \\ & + C_{j4} \Phi_4'(1s^2 2s^2 2p^6 3s 3p^4(3P)^2 P 3d^2(3P)) + C_{j5} \Phi_5'(1s^2 2s^2 2p^6 3s 3p^4(3P)^2 P 3d^2(3P)). \end{aligned} \quad (15)$$

TABLE I. MCHF  $\langle nl' | nl \rangle$  overlap integrals for  ${}^4\text{Be}$  electron capture.

	K capture			L <sub>1</sub> capture	
	1s)	2s)	2p)	1s)	2s)
$\langle 1s'  $	0.972 09	-0.190 99		0.962 47	-0.155 91
$\langle 2s'  $	0.171 93	0.967 85		0.082 71	0.882 83
$\langle 2p'  $			0.992 60		

TABLE II. MCHF  $\langle nl' | nl \rangle$  overlap integrals for  $^{18}\text{Ar}$  electron capture.

	$ 1s\rangle$	$ 2s\rangle$	$ 2p\rangle$	$ 3s\rangle$	$ 3p\rangle$	$ 3d\rangle$
$L_1$ capture						
$\langle 1s'  $	0.998 73	-0.029 77		-0.006 30		
$\langle 2s'  $	0.027 05	0.992 50		-0.104 96		
$\langle 2p'  $			0.998 58		-0.022 79	
$\langle 3s'  $	0.007 98	0.101 77		0.992 74		
$\langle 3p'  $			0.021 42		0.999 27	
$\langle 3d'  $						0.999 54
$M_1$ capture						
$\langle 1s'  $	0.998 75	-0.029 21		-0.006 28		
$\langle 2s'  $	0.026 23	0.992 28		-0.097 36		
$\langle 2p'  $			0.994 45		-0.081 77	
$\langle 3s'  $	0.00702	0.090 20		0.989 13		
$\langle 3p'  $			0.075 52		0.990 47	
$\langle 3d'  $						0.932 00

TABLE III. Electron radial wave-function ratios  $R_{ns}^2(0)/R_{n's}^2(0)$ , exchange-overlap correction factors  $B_i$ , and capture ratios  $\lambda_i/\lambda_j$ .

Element	Quantity	Result	
$^7\text{Be}$	$R_{2s}^2(0)/R_{1s}^2(0)$ , HF	0.0332	
		MCHF <sup>c</sup>	0.0300
	$B_K$ , HF(V) <sup>a</sup>	0.816	
		HF(B) <sup>b</sup>	0.900
		MCHF <sup>c</sup>	0.792
	$B_L$ , HF(V) <sup>a</sup>	2.222	
		HF(B) <sup>b</sup>	3.045
		MCHF <sup>c</sup>	2.259
	$\lambda_L/\lambda_K$ , HF(V) <sup>a</sup>	0.090	
		HF(B) <sup>b</sup>	0.112
		MCHF <sup>c</sup>	0.086
	$^{37}\text{Ar}$	$R_{3s}^2(0)/R_{2s}^2(0)$ , HF	0.0977
MCHF <sup>c</sup>			0.0669
$B_L$ , HF(V) <sup>a</sup>		1.121	
		HF(B) <sup>b</sup>	1.171
		MCHF <sup>c</sup>	1.098
$B_M$ , HF(V) <sup>a</sup>		1.322	
		HF(B) <sup>b</sup>	1.549
		MCHF <sup>c</sup>	1.674
$\lambda_M/\lambda_L$ , HF(V) <sup>a</sup>		0.115	
		HF(B) <sup>b</sup>	0.129
		MCHF <sup>c</sup>	0.102
		Experiment <sup>d</sup>	$0.104^{+0.007}_{-0.003}$

<sup>a</sup>Hartree-Fock, Vatai's approach (Refs. 2 and 9).<sup>b</sup>Hartree-Fock, Bahcall's approach (Refs. 2 and 3-6).<sup>c</sup>Present multiconfigurational HF calculation.<sup>d</sup>Ref. 11.

The MCHF wave functions, including the amplitudes  $C$ , were computed with the Froese Fischer program.<sup>7</sup> The electrostatic interaction matrix elements were calculated with Hibbert's program.<sup>10</sup> The one-electron overlap integrals are listed in Tables I and II. The electron radial-wave-function ratios at the origin and the overlap-exchange correction factors  $B_i$  as well as the electron-capture ratios are listed in Table III. For comparison, theoretical single-configuration HF capture ratios<sup>2</sup> and the experimental result<sup>11</sup> for  $^{37}\text{Ar}$  are also listed; there is no measurement of the  $^7\text{Be}$   $L/K$  ratio.

Electron correlation is seen to have a substantial effect on nuclear capture ratios when outer electrons are involved. Compared with single-configuration HF results according to Vatai's approach,<sup>2</sup> the MCHF  $L/K$  capture ratio of  $^7\text{Be}$  is reduced by 4.4%; the  $^{37}\text{Ar}$   $M/L$  ratio is reduced by 11% and brought into excellent agreement with experiment.<sup>2,11</sup>

This work was supported in part by the U. S. Army Research Office under Grant No. DAAG29-78-G-0010 and by the National Aeronautics and Space Administration under Grant No. NGR 38-003-036.

<sup>1</sup>P. Benoist-Gueutal, C. R. Acad. Sci. **230**, 624 (1950).<sup>2</sup>For a recent review, see W. Bambynek, H. Behrens, M. H. Chen, B. Crasemann, M. L. Fitzpatrick, K. W. D. Ledingham, H. Genz, M. Mutterer, and R. L. Intemann, Rev. Mod. Phys. **49**, 78 (1977).

- <sup>3</sup>J. N. Bahcall, Phys. Rev. Lett. **9**, 500 (1962).  
<sup>4</sup>J. N. Bahcall, Phys. Rev. **129**, 2683 (1963).  
<sup>5</sup>J. N. Bahcall, Phys. Rev. **131**, 1756 (1963).  
<sup>6</sup>J. N. Bahcall, Nucl. Phys. **71**, 267 (1965).  
<sup>7</sup>C. Froese Fischer, Comput. Phys. Commun. **4**, 107 (1972).

- <sup>8</sup>H. Brysk and M. E. Rose, Rev. Mod. Phys. **30**, 1169 (1958).  
<sup>9</sup>E. Vatai, Nucl. Phys. **A156**, 541 (1970).  
<sup>10</sup>A. Hibbert, Comput. Phys. Commun. **2**, 180 (1971).  
<sup>11</sup>J. P. Renier, H. Genz, K. W. D. Ledingham, and R. W. Fink, Phys. Rev. **166**, 935 (1968).

## Population of Resonant $^{12}\text{C}+^{12}\text{C}$ States via the Reaction $^{12}\text{C}(^{16}\text{O}, \alpha)^{24}\text{Mg}$

A. J. Lazzarini, E. R. Cosman, A. Sperduto, S. G. Steadman, W. Thoms, and G. R. Young  
*Laboratory for Nuclear Science, Massachusetts Institute of Technology, Cambridge, Massachusetts 02139*

(Received 10 November 1977)

Excitation functions for the reaction  $^{12}\text{C}(^{16}\text{O}, \alpha)^{24}\text{Mg}$  have been measured from  $E_{\text{lab}}(^{16}\text{O}) = 62$  to 110 MeV using a counter telescope at  $\theta_{\text{lab}} = 7.5^\circ$ . Selective population of relatively few states at very high excitation energies in  $^{24}\text{Mg}$  [ $E_x(^{24}\text{Mg}) > 20$  MeV] is seen. A possible correspondence is found between these states and the narrow resonances reported in  $^{12}\text{C} + ^{12}\text{C}$  reactions. In addition, a possible correspondence between averaged yields in  $^{12}\text{C}(^{16}\text{O}, \alpha)^{24}\text{Mg}$  and gross structure seen in several  $^{12}\text{C} + ^{12}\text{C}$  reaction channels is cited.

The reaction  $^{12}\text{C}(^{16}\text{O}, \alpha)^{24}\text{Mg}$  has been studied extensively because of its striking final-state selectivity. It is interesting to consider whether this behavior reflects special structures in the initial, compound, and final systems. In this work we have significantly extended the  $^{12}\text{C}(^{16}\text{O}, \alpha)^{24}\text{Mg}$  excitation functions. An apparent correlation has been found between individual pronounced transitions in that reaction and resonant states which have been seen in  $^{12}\text{C} + ^{12}\text{C}$  reactions. Furthermore, the envelope of the  $^{12}\text{C}(^{16}\text{O}, \alpha)^{24}\text{Mg}$  transitions shows a weak correlation with gross structure variations in the  $^{12}\text{C}$  strength function as indicated by several  $^{12}\text{C} + ^{12}\text{C}$  reaction-channel excitation functions.

High-resolution spectra from the reaction  $^{12}\text{C}(^{16}\text{O}, \alpha)^{24}\text{Mg}$  were measured from  $E_{\text{lab}}(^{16}\text{O}) = 62.0$  to 100.0 MeV in 1-MeV steps. Two measurements at  $E_{\text{lab}}(^{16}\text{O}) = 105.0$  and 110.0 MeV were also taken. The experiment was performed at the Brookhaven National Laboratory Tandem Van de Graaff facility and employed a surface-barrier counter telescope placed at  $\theta_{\text{lab}} = 7.5^\circ \pm 0.25^\circ$ . Targets were nominally  $45\text{-}\mu\text{g}/\text{cm}^2$  natural carbon. The experimental resolution was typically 90 keV.

The primary objective of the study was to determine if the  $^{12}\text{C}(^{16}\text{O}, \alpha)^{24}\text{Mg}$  spectra at higher energies show any gross- or fine-structure correlations to previously known  $^{24}\text{Mg}$  states which have been observed via  $^{12}\text{C} + ^{12}\text{C}$  resonance reactions. The  $\alpha$  spectra contain numerous previously unseen transitions in the range of  $E_x(^{24}\text{Mg}) = 20$  to 35 MeV—a region in which most  $^{12}\text{C} + ^{12}\text{C}$  reso-

nances have been recorded. The  $\alpha$ -transition yields exhibit compound-nuclear fluctuations; to average out this effect and to enhance the persistently strong transitions, the spectra were averaged over the incident  $^{16}\text{O}$  energy. This was performed by linearizing the 39 individual  $\alpha$  spectra to a common  $^{24}\text{Mg}$  excitation-energy scale. Kinematic corrections were performed so the energy-summed spectra would reflect center-of-mass cross sections. A smooth evaporative background was subtracted by hand from each spectrum to further enhance strong discrete transitions in the summed spectra. Figure 1 shows three typical linearized spectra and background curves. It is understood that the magnitude of the underlying

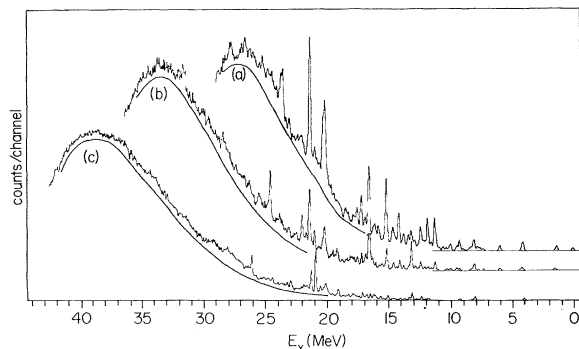


FIG. 1. Typical  $^{12}\text{C}(^{16}\text{O}, \alpha)^{24}\text{Mg}$  spectra at  $E_{\text{lab}} = 63$  (curve a), 77 (curve b), and 91 MeV (curve c). They have been linearized in  $E_x(^{24}\text{Mg})$  and the smooth curves are hand drawn to represent the background that is to be subtracted.